Oral Absorption Enhancement of Cromolyn Sodium Through Noncovalent Complexation

Xuan Ding,[1] Parshuram Rath,[2] Robert Angelo,[2] Thomas Stringfellow,[1] Elizabeth Flanders,[2] Steven Dinh,[2] Isabel Gomez-Orellana,[2] and Joseph R. Robinson[1]

Received May 23, 2004; accepted August 26, 2004

Purpose. To determine the effect of Sodium *N*-[8-(2-hydroxybenzoyl)amino]caprylate (SNAC) on the permeation of cromolyn across Caco-2 cell monolayers and explore the molecular basis for the enhanced absorption.

Methods. Transport studies of cromolyn across Caco-2 cell monolayers were conducted in the presence of various SNAC concentrations. Permeation of cellular transport markers and lactate dehydrogenase (LDH) release were measured to evaluate cell integrity. Molecular interactions betweent the two compounds were investigated using isothermal titration calorimetry (ITC), nuclear magnetic resonance (NMR), and Fourier-transfrom infrared (FTIR) spectroscopies and molecular dynamics simulations.

Results. The absorption of cromolyn across Caco-2 monolayers was enhanced markedly by SNAC. SNAC did not cause significant LDH leakage and changes in the permeation of transport markers. ITC, spectroscopies, and molecular dynamic simulations indicated the existence of intermolecular interactions between cromolyn and SNAC that involve the 2-hydroxybenzamide moiety on SNAC and weaken the hydrogen bonding between cromolyn and surrounding water molecules.

Conclusions. SNAC increases the permeability of Caco-2 monolayers to cromolyn without measurable cell damage. SNAC interacts with cromolyn mainly via ring stacking. One major mode of interaction appears to involve the insertion of the aromatic ring of SNAC between cromolyn's rings. Such interaction appears to reduce the hydration of cromolyn and thus optimize its hydrophobicity for oral absorption.

KEY WORDS: Caco-2 monolayers; cromolyn sodium; isothermal titration calorimetry; NMR.

INTRODUCTION

Cromolyn sodium (Scheme 1), also known as disodium cromoglycate, has been used for the treatment of allergic diseases, such as bronchial asthma and allergic rhinitis, since the mid-1970s (1). For these indications, the drug is administered locally by inhalation or as an intranasal solution. The pharmacology of cromolyn is based on its ability to inhibit the degranulation of sensitized pulmonary mast cells that occurs upon exposure to certain antigens (2). Adverse effects documented in humans are minimal, reversible, and limited to transient irritation at local dosing sites. Although, at present, sufficient efficacy for these indications is achieved by local administration, an oral formulation of cromolyn would be desirable as it would improve patient compliance and eliminate dose delivery variability associated with local dosing. In addition, oral formulations of cromolyn would open the door for the development of systemic treatments for a broad range of inflammatory diseases. At present, the oral bioavailability of cromolyn is less than 1% (3). Several cromolyn prodrugs have been designed in an attempt to improve the oral absorption of cromolyn (4,5). These studies have shown promising results in animal models, but further development is still needed.

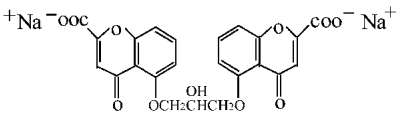

Cromolyn Sodium

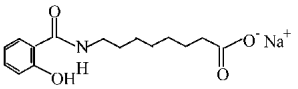

SNAC

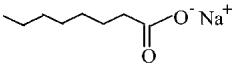

Sodium Caprylate

Scheme 1. Chemical structures of cromolyn sodium, SNAC, and sodium caprylate.

Over the past few years, a series of novel drug delivery agents have been developed that enable oral absorption of macromolecular drugs, such as human growth hormone (6,7), insulin (8), parathyroid hormone (9), and heparin (10,11). Results from various studies indicated that these delivery agents enhance drug absorption by interacting noncovalently with the drugs to increase their hydrophobicity (8,9,12). These delivery agents neither chemically alter the compounds to be transported nor interfere with any identified active cellular transporters (7,13). Mechanistic studies have shown that these delivery agents do not inflict detectable macroscopic or microscopic damage on the intestinal epithelium (6,7,10, 14,15). Moreover, pretreatment of cells with delivery agents followed by a thorough washout does not provide effective drug absorption (7).

In the mid-1990s, it was found that the oral bioavailability of cromolyn could be increased 8-fold when the drug was coadministered with these delivery agents in a rat model (12). The same study suggested that the hydrophobic nature of non-covalent complexes between the delivery agents and cromolyn was responsible for the increase in cromolyn absorption across the gastrointestinal wall. No pathology was observed in the gastrointestinal tract of dosed animals. Recent clinical studies confirmed the ability of these delivery agents to enhance the oral absorption of cromolyn in humans (16).

In this study, we investigated the mechanism of oral absorption of cromolyn in the presence of an oral delivery agent, sodium *N*-[8-(2-hydroxybenzoyl)amino]caprylate (SNAC). Caco-2 cell monolayers were used to study the transport pathways and the effect of SNAC on the epithelium. The interaction between cromolyn and SNAC and its impact on the oral absorption of cromolyn were studied using isothermal titration calorimetry (ITC), nuclear magnetic resonance

[1] School of Pharmacy, University of Wisconsin-Madison, Madison, Wisconsin 53705, USA.
[2] Emisphere Technologies, Inc.
[3] To whom correspondence should be addressed. (e-mail: jrrobinson@pharmacy.wisc.edu)

0724-8741/04/1200-2196/0

(NMR), Fourier-transform infrared (FTIR) spectroscopies and molecular modeling.

MATERIALS AND METHODS

Materials

Caco-2 cells originating from a human colorectal carcinoma were obtained from American Type Culture Collection (Manassas, VA, USA). Cromolyn sodium was purchased from Interchem Co. (Paramus, NJ, USA). Dulbecco's Modified Eagle Medium (DMEM), Hank's balanced salt solution (HBSS), fetal bovine serum, nonessential amino acids, penicillin, and streptomycin were purchased from Invitrogen (Carlsbad, CA, USA). SNAC was synthesized at Emisphere Technologies, Inc. (Tarrytown, NY, USA). Two different types of deuterium oxide (D_2O; 99.9 atom % D) were obtained from Aldrich Chemical Co. (Milwaukee, WI, USA): D_2O with 0.05 weight % sodium salt of TSP (3-(trimethylsilyl) propionic-2,2,3,3-d_4 acid) as an internal NMR chemical shift reference, and D_2O without TSP used in FTIR measurements. All other chemicals were from Sigma (St. Louis, MO, USA). The CytoTox 96 kit was obtained from Promega (Madison, WI, USA).

Cell Culture

Caco-2 cells of passage number 20 to 40 were seeded on polycarbonate filters, TRANSWELL cell culture inserts (Costar, Cambridge, MA, USA) of 0.45-μm pore size and 24.5-mm diameter. Cells were cultured at 37°C and 5% CO_2 atmosphere in DMEM growth medium supplemented with 10% (v/v) fetal bovine serum, 1% (v/v) nonessential amino acids, penicillin (100 unit/mL), and streptomycin (100 μg/mL) until fully differentiated on 21 to 25 days. The integrity of the Caco-2 monolayers was determined by measuring the transepithelial electrical resistance (TEER) with an Epithelial Voltohmmeter EVOM-G (World Precision Instruments, Sarasota, FL, USA) and a pair of silver/silver-chloride pellet electrodes. Only cell monolayers with an initial TEER value above 200 Ω/cm^2 were used.

Solution Preparation

For the NMR measurements, cromolyn and/or SNAC were dissolved in D_2O or in D_2O/H_2O (10/90 v/v). The pDs of all the solutions in pure D_2O were measured between 7.2 and 7.6 at 25°C; within this range, any influence of pD variation on the spectral properties was found to be insignificant. Sodium or potassium chloride was dissolved directly in the sample solution to investigate the ionic effect on molecular interaction; solution pDs were adjusted with 0.1 M HCl or 1 M NaOH at 25°C to examine this effect. As 83 mM SNAC greatly improves the buffering capacity of the 10 mM cromolyn solution, a much larger amount of NaOH was required to significantly increase the pD of the mixture. Under such circumstances, the Na^+ effect on the spectral properties of cromolyn was not negligible. Therefore, certain volumes of 1 M NaOH (i.e., 40 and 60 μL) were added to 1 mL of the mixture to achieve pD 8.8 and 9.9, respectively. The excess Na^+ concentrations in the mixtures were calculated at 40 and 60 mM, respectively. Thus, the effect of Na^+ from NaOH can be predicted from spectra of mixtures containing NaCl at comparable concentrations.

For the FTIR experiments, cromolyn and/or SNAC solutions were prepared in D_2O in a dry cabinet under a nitrogen atmosphere.

Transport Experiments

For transport experiments, six well plates containing Caco-2 monolayers on TRANSWELL filters were mounted on an orbital shaker at 30–40 rpm and 37°C in an atmosphere of 5% CO_2. The seeding density was 80,000 cells/cm^2. The growth medium was removed and the cells were washed three times with HBSS and incubated for 20 min in HBSS buffer, pH 7.4. Afterwards, the apical solution was replaced with HBSS containing cromolyn and SNAC or the compounds used in control experiments (theophylline, fluorescein, sodium caprylate). Cromolyn, theophylline and fluorescein concentrations were kept at 10 mM in all transport experiments. SNAC concentration was varied from 17 to 83 mM. Aliquots of 200 μL were taken from the basolateral solution every 15 min and replaced with an equal volume of HBSS. The duration of each experiment was 120 min. The concentration of cromolyn or theophylline in the basolateral solutions was measured by HPLC. Sodium fluorescein was quantified by measuring absorbance at 490 nm on a MRX TC Revelation absorbance microplate reader (DYNEX Technologies, Chantilly, VA, USA). The apparent permeability coefficient (Papp) was calculated using the following equation:

$$\text{Papp} = V/(A \cdot C_0) \cdot dC/dt$$

where dC/dt is the flux across the monolayer, V is the volume of the basolateral solution (2.5 mL), A is the monolayer surface area (4.71 cm^2), and C_0 the initial concentration in the apical solution. Statistical differences between the means based on 3–6 monolayers for each mean calculation were evaluated using Student's *t* test.

High-Performance Liquid Chromatography (HPLC)

Cromolyn and theophylline concentrations in the basolateral solutions were determined by HPLC. The system was composed of a Hitachi L-6200 Intelligent Pump, a Perkin-Elmer ISS100 Autosampler, a MetaTherm column heater (MetaChem Technologies, Lake Forest, CA, USA), and a Perkin-Elmer LC-96 UV-Vis Detector. A 5 μL sample of each aliquot was injected onto a Zorbax SB-C18 Rapid Resolution cartridge (2.1 × 30 mm, 3.5 μm, Agilent Technologies, Palo Alto, CA, USA). The column was maintained at 40°C throughout the run. The mobile phase consisted of a mixture of deionized water and acetonitrile with 0.1% acetic acid. An initial gradient of 5–95% acetonitrile (1 mL/min) was adjusted to optimize the elution of each individual compound of interest. Detection was at 244 nm. Running time was 6 min. This method ensured reproducible and rapid separation of cromolyn, theophylline, SNAC, and caprylate. The retention times of these compounds were 1.5, 0.8, 2.3, and 2.2 min, respectively.

Lactate Dehydrogenase (LDH) Release

LDH is a stable cytosolic enzyme that is released upon cell membrane damage. The CytoTox 96 Assay was used to quantitatively measure LDH released from Caco-2 cells during cromolyn permeation. Absorbance was read at 490 nm on

the MRX TC Revelation absorbance microplate reader. The positive control was monolayers treated with 1% Triton X-100 for up to 120 min. Fifty μL of solutions were collected from the basolateral solutions every 15 min. Complete cell lysis (100% LDH released) was assumed at 120 min. The percentage of LDH released during the transport process was calculated as the ratio of absorbance of the specific basolateral aliquot to absorbance upon complete lysis with Triton X-100.

Isothermal Titration Calorimetry

Calorimetric experiments were carried out on a VP-ITC microcalorimeter (MicroCal, Northampton, MA, USA) at 25.0 ± 0.5°C. The sample cell was filled with approximately 2 mL of 15 mM cromolyn and titrated with 150 mM SNAC or caprylate using the automated rotating stirrer-syringe at constant time intervals of 6 min. All solutions were prepared in 10 mM sodium phosphate buffer at pH 7.5. The titrants were added stepwise to the cromolyn solution in aliquots of 4 μL. The heat of reaction obtained after each injection was corrected for the heat of dilution of titrants and cromolyn, which were determined in separate experiments by titrating cromolyn with buffer or the titrants nto buffer. The data were processed using the software Origin (MicroCal, Origin Lab Co.).

Nuclear Magnetic Resonance Spectroscopy

NMR measurements were performed on Varian UNITY INOVA model spectrometers (Varian Inc., Palo Alto, CA, USA) operating at 400 and 500 MHz nominal proton frequencies, at 25°C. Sample temperature was regulated for all measurements. Each spectrometer was equipped with an FTS Systems preconditioning device (comprised of a refrigeration unit, internal temperature controller and insulated transfer line) to control pre-cooling or preheating of the compressed and dried air used as a temperature control medium; final temperature regulation of the sample is achieved within the NMR probe. Acquisition parameters were adjusted on a case-by-case basis to provide adequate signal-to-noise and spectral resolution, the latter typically at 0.5 and 4.2 ppb/point for 1D high-resolution ^{1}H and ^{13}C spectra, respectively. Carbon-13 spectra were acquired with proton decoupling. All ^{1}H and ^{13}C spectra were referenced with respect to TSP at 0.0 ppm. For samples dissolved in D_2O/H_2O (10/90 v/v), the WET (Water Elimination by Transverse Gradients) sequence (17,18) was used to suppress the intense water resonance. One-dimensional ^{1}H homonuclear Overhauser effect spectra were based upon the "double pulsed field gradient spin-echo" sequence as a means of selecting a target resonance from which the nuclear Overhauser effects (NOEs) ultimately develop (19–21). The mixing time τ_m was fixed at 1 s, comparable to the longitudinal relaxation times (T_1s) of the ^{1}H resonances.

Fourier-Transform Infrared Spectroscopy

Infrared measurements were carried out on a nitrogen gas purged BioRad FTS 175C FTIR spectrometer (BioRad Laboratories, Hercules, CA, USA) equipped with a mid-IR DTGS detector. Spectra were recorded by averaging 256 scans collected at a resolution of 2 cm^{-1} in the range of 1000–4000 cm^{-1}, using a horizontal ATR detection equipped with a ZnSe trough. The spectra were processed with WIN-IR software (BioRad) to minimize moisture bands, subtract solvent (baseline) spectra and isolate single-component spectra in a mixture.

Molecular Modeling

Molecular dynamics simulations were performed in the NVE ensemble (22,23) at 300 K using C^2Dynamics (Accelrys, Inc., San Diego, CA, USA). The force field was cff01.1. Dynamics simulations of 0.5–1 ns were recorded (1fs/step) after equilibrating the system for ~0.1 ns. Preliminary short simulations (0.5 ns) were done both with and without explicit solvation water to test whether there were significant differences between these two conditions. Initial simulations performed with explicit solvation water rendered results comparable to those performed without solvation water but with a dielectric constant of 80. Thus, to reduce computational time, simulations were carried out without explicit water. The starting system contained one molecule of cromolyn and one molecule of SNAC separated by 8–15 Å. Some simulations were also done with two molecules of cromolyn and two molecules of SNAC. Simulations were done starting with either an extended conformation of cromolyn or a conformation of cromolyn obtained after molecular dynamics simulations and energy minimization, in which cromolyn is slightly bent and the two aromatic rings are facing each other, as in the conformation found in cromolyn's crystal structure (24).

RESULTS

Cromolyn Transport Across Caco-2 Monolayers

Cromolyn was undetectable in the basolateral solutions of Caco-2 monolayers incubated with cromolyn alone or with cromolyn and 17–51 mM SNAC (detection limit by HPLC ~1 μg/mL). However, in the presence of 67 and 83 mM SNAC, cromolyn permeation was measurable and increased with SNAC concentration (Fig. 1).

In order to determine whether SNAC functions as a classic absorption enhancer (i.e., membrane damage) or by an

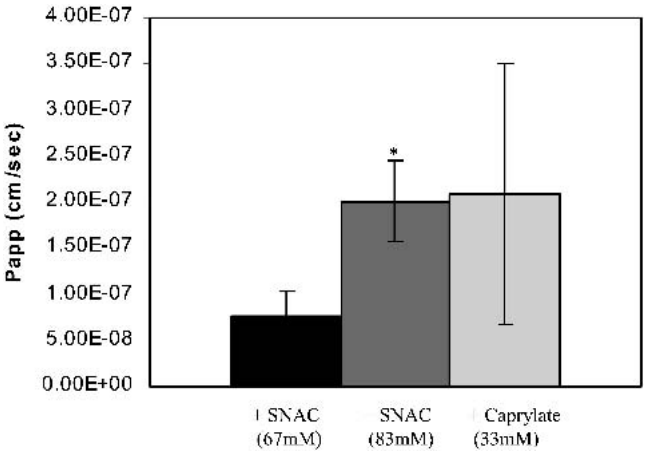

Fig. 1. Cromolyn sodium (10 mM) permeation in the presence of SNAC or sodium caprylate (n = 3 to 6, * denotes statistical significance of $p < 0.05$ compared to "+ 67 mM SNAC"). No cromolyn was detected in the basolateral solutions when monolayers were incubated with cromolyn alone, yielding Papp = 0 cm/s.

alternate mechanism, a direct comparison between SNAC and a known absorption enhancer, sodium caprylate, was performed. Sodium caprylate caused an increase in cromolyn absorption comparable to that of SNAC but showed high variability (Fig. 1). This high variability in Caco-2 permeability to cromolyn sharply contrasts with that observed with SNAC and may be an indication of differences in the underlying mechanism of action of these two compounds.

Effect of SNAC on the Permeation of Paracellular and Transcellular Markers

Sodium fluorescein was chosen as a marker to assess the effect of SNAC on paracellular transport. No increase in fluorescein permeation was observed in the presence of SNAC, although a slight decrease was observed in the presence of 67 mM SNAC (Fig. 2). In contrast, sodium caprylate gave a sharp increase in fluorescein concentration in the basolateral solutions at very early time points. This made any determination of fluorescein permeability coefficient impractical. This high fluorescein absorption seemed more indicative of monolayer leakage than of a controlled absorption process.

Theophylline was used as a marker molecule to assess the effect of SNAC on the transcellular pathway. SNAC did not alter theophylline's permeation. In contrast, sodium caprylate significantly increased theophylline permeation (Fig. 3).

LDH Release

LDH release into the basolateral solutions during cromolyn absorption in the presence of 67 and 83 mM SNAC was comparable to that observed in the absence of the delivery agent (Fig. 4). A slight increase in LDH release was observed in the last time point, near the viability limit of the monolayers in HBSS (2 h). The absorption of cromolyn, however, occurred through the earlier time points, which were the ones that determined the permeability coefficients. These results indicate that the absorption of cromolyn occurred without causing measurable membrane damage. This is consistent with the observed lack of permeation increase of paracellular and transcellular markers in the presence of these SNAC concentrations. Any cell membrane damage would have resulted

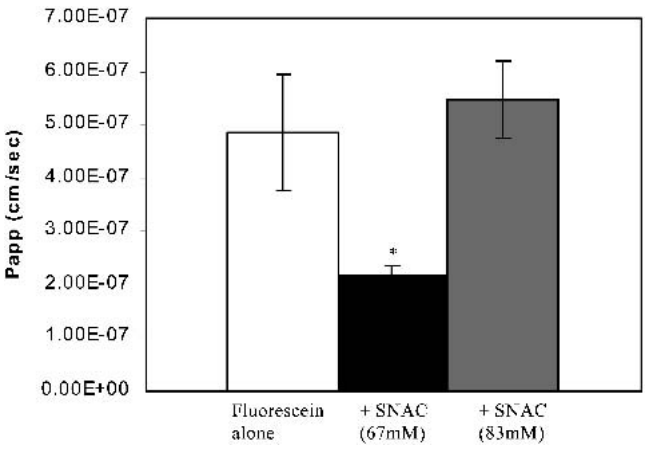

Fig. 2. Sodium fluorescein (10 mM) permeation in the absence and presence of SNAC (n = 3 to 6, * denotes statistical significance of $p < 0.05$ compared to "fluorescein alone").

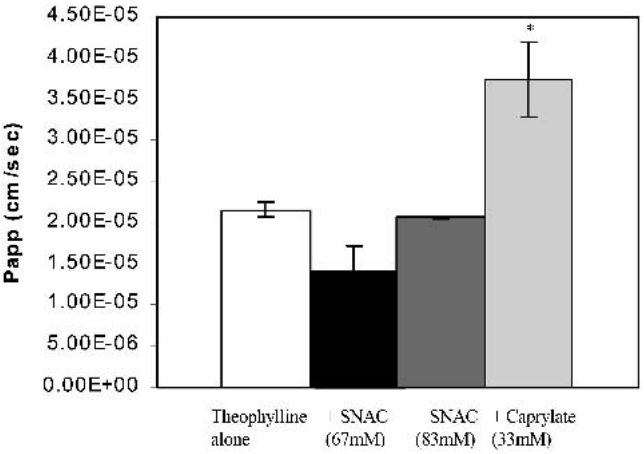

Fig. 3. Theophylline (10 mM) permeation in the absence and presence of SNAC or sodium caprylate (n = 3 to 6, * denotes statistical significance of $p < 0.05$ compared to "theophylline alone").

in an increase in permeation of paracellular and transcellular markers, which was not observed in our experiments. It was surprising that under our experimental conditions, caprylate did not cause significant LDH release from the monolayers. However, caprylate showed great impact on the permeation of paracellular and transcellular markers (i.e., fluorescein and theophylline).

ITC

The molecular interaction between cromolyn and SNAC was first characterized by isothermal titration calorimetry. Figure 5A shows the calorimetric traces obtained after addition of successive amounts of a SNAC solution into a cromolyn solution, as well as, those corresponding to the controls, that is, addition of SNAC into buffer and addition of buffer into cromolyn, under the same conditions. The heat effect obtained upon mixing SNAC and cromolyn could not be accounted for by the sum of the heat of dilution of SNAC and cromolyn (control experiments). This clearly indicates the existence of interactions between cromolyn and SNAC. When the same calorimetric experiments were performed with sodium caprylate instead of SNAC (Fig. 5B), no difference was observed between the heat of mixing caprylate and cromolyn and the sum of the control dilution experiments. This indicates a lack of intermolecular interaction between

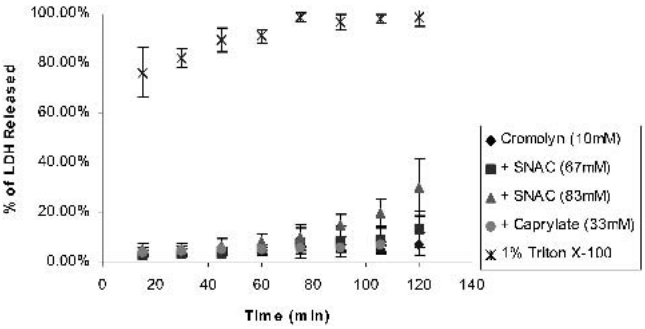

Fig. 4. Lactate dehydrogenase (LDH) released from Caco-2 cells treated with Triton X-100, cromolyn in the absence and presence of SNAC or sodium caprylate during transport processes. Each percentage was the average value calculated from 3 to 6 monolayers.

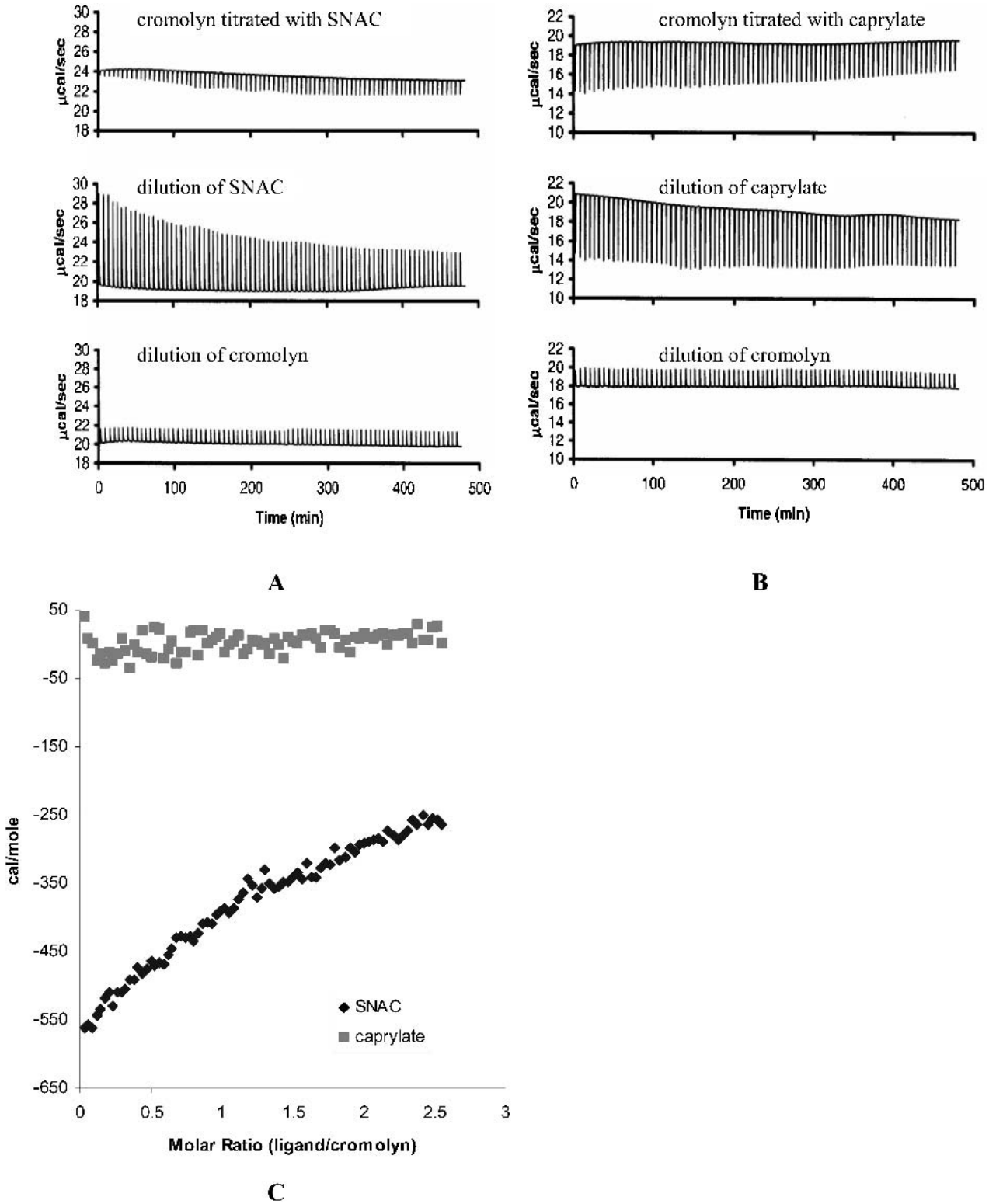

Fig. 5. Calorimetric traces obtained during titration of cromolyn with SNAC (A) or caprylate (B) and the corresponding blank experiments. (C) Comparison of normalized titration curves obtained for SNAC and caprylate after subtraction of the blanks.

caprylate and cromolyn. Figure 5C shows the titration curves obtained from the cromolyn/SNAC and cromolyn/caprylate experiments. Each data point on the graph corresponds to the heat obtained in each titration step, after correction for the corresponding heats of dilution obtained in the control experiments. No titration curve was obtained from the cromolyn/caprylate experiment because the heat in all titration steps was zero, indicating no interaction between these two compounds. The titration curve obtained from the cromolyn/SNAC experiment, on the other hand, shows a gradual heat

change as a function of the SNAC:cromolyn ratio, typical of intermolecular interactions. The curve does not reach a plateau at values near zero within the SNAC:cromolyn ratio of the experiment. This is indicative of a weak interaction and possibly of the presence of more than one type of interaction between these two molecules. It was not possible to determine the binding constant/s and number of binding sites or binding types with accuracy from this titration curve because of the weakness of the interaction.

Scheme 1 shows the structures of SNAC and sodium caprylate. The difference between these two compounds lies in the 2-hydroxybenzamide group of SNAC. Because there is no interaction between caprylate and cromolyn, it can therefore be concluded that the 2-hydroxybenzamide moiety is involved in cromolyn/SNAC interaction.

Proton NMR

In the 1D ^{1}H NMR spectra of cromolyn (Fig. 6A), the resonances in the 6.5–7.5 ppm region are due to the eight CH protons symmetrically located on the rings; the resonances between 4.2 and 4.6 ppm are due to the isopropyl linkage between the two rings. The lone cromolyn hydroxyl resonance was not observed in a D_2O/H_2O mixture (spectra not shown), owing to rapid exchange with solvent and consequent coalescence into the solvent peak at 4.8 ppm. In our earlier NMR study (25) of cromolyn in aqueous solution, we observed that all the cromolyn ^{1}H resonances displayed spectral upfield shifts (more shielded) with increasing concentration, which was explained by an intermolecular, ring-stacking driven self-association. Such a universal upfield shift was not observed when cromolyn was mixed with various amounts of SNAC (Figs. 6B, 6C). In the presence of SNAC, H7 of cromolyn shifted upfield, whereas the H3 resonance shifted downfield. Resonances of cromolyn's H6 and two ring protons of SNAC largely overlapped, but this cluster of resonances shifted upfield when SNAC concentration increased.

In our earlier NMR study of cromolyn solution (25), we noticed a marked line broadening in concentrated cromolyn solutions due to a pronounced reduction in the molecular mobility resulting from liquid crystal formation. The presence of additional Na^+ intensified this effect, resulting in even broader lines. However, in the present study we found that when mixed with 167 mM SNAC, the broad resonances observed at high cromolyn concentrations (120 mM) were narrowed sufficiently to recover the ^{1}H multiplicity (Fig. 7).

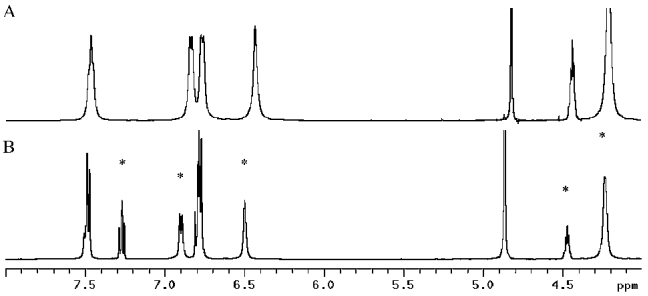

Fig. 7. ^{1}H NMR spectra of 120 mM cromolyn (A), mixed with 167 mM SNAC (B). Cromolyn peaks are marked by * in B.

In the 1D ^{1}H NMR spectra of SNAC (Fig. 8A), the resonances between 6 and 8 ppm are assigned to the four CH aromatic protons. The triplet at 2.2 ppm is due to the CH_2 next to the carboxyl group; the CH_2 proton next to the amide gives the resonance around 3.4 ppm. The upfield multiplets are due to the remaining CH_2 aliphatic protons H3–H7. The small, broad resonance at 8.8 ppm is due to the –NH proton. As shown in Fig. 8B, addition of cromolyn caused an upfield shift (i.e., more shielded) of 2-hydroxylbenzamide proton as well as H8 on SNAC. The rest of the aliphatic protons were barely affected.

Table I shows the effects of electrolyte and pD on cromolyn's spectral shifts obtained in the presence of SNAC. Sodium and potassium chloride both caused upfield shifts of H7, H8 and a relatively small change on H3. Investigation of the pD effect on the interaction was restricted by the low solubility of SNAC below pD 7.3. Within the pD range studied, no changes were observed on the H7 resonance. H3 and H8 shifted slightly to lower frequencies with increasing pH. The H6 resonance resolved in basic pDs but did not shift. The effects of NaCl, KCl and pD on cromolyn proton chemical shifts are markedly different from those observed under the

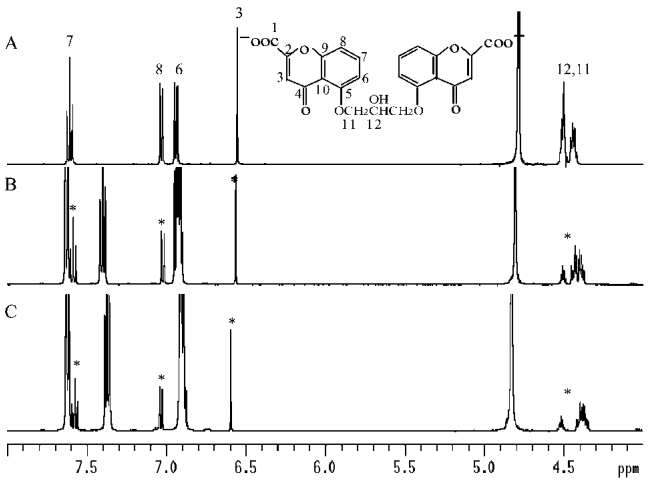

Fig. 6. ^{1}H NMR spectra of 10 mM cromolyn (A), mixed with 83 mM (B) or 167 mM (C) SNAC in D_2O. Cromolyn peaks are marked by * in B and C.

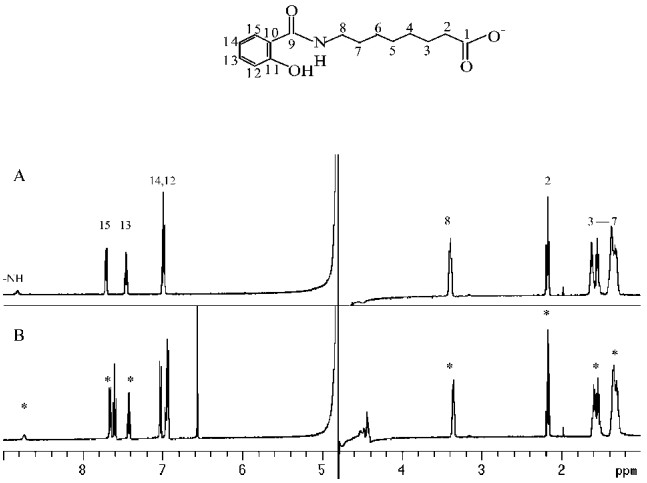

Fig. 8. ^{1}H NMR spectra of 17 mM SNAC (A), mixed with 10 mM cromolyn (B) in 10% D_2O/90% H_2O. SNAC peaks are marked by * in B.

Table I. Ion and pD Effects on ^{1}H Chemical Shifts (ppm) of Cromolyn (10 mM) in the Presence of SNAC (83 mM)

		$[Na^+Cl^-]$ (M) in the solution				$[K^+Cl^-]$ (M) in the solution				pD	
^{1}H δ	∅	0.05	0.1	0.2	0.4	0.05	0.1	0.2	0.4	8.8	9.9
H3	6.565	6.564	6.563	6.562	6.561	6.561	6.560	6.557	6.552	6.557	6.552
H6	NA	NA	NA	NA	NA	NA	NA	NA	NA	6.908	6.908
H7	7.586	7.579	7.575	7.568	7.555	7.581	7.577	7.568	7.556	7.586	7.585
H8	7.022	7.016	7.013	7.007	6.998	7.016	7.013	7.006	6.996	7.016	7.013

∅: 10 mM cromolyn and 83 mM SNAC in D_2O without extra monovalent ions added, pD = 7.3.

same conditions in the absence of SNAC. In the absence of SNAC, pD (range from 3.5 to 11.7) had no effect on cromolyn's proton resonances and an increase in NaCl or KCl concentration caused a substantial shielding of proton resonances (25).

Carbon-13 NMR

Table II shows the influence of SNAC on cromolyn ^{13}C NMR chemical shifts. Significant upfield shifts occurred to C6 and C7 as well as aliphatic carbons. C5, the closest quarternary ^{13}C neighbor of the isopropyl linkage was the most affected, followed by the carbonyl C4. In contrast, the carbons closer to the charged groups but relatively distant from the isopropyl linkage, such as C2 and C3, were overall less affected. Little perturbation occurred to the carboxyl ^{13}C.

Table III shows that the 2-hydroxybenzamide carbon resonances of SNAC experienced significant upfield shifts in the presence of cromolyn, similar to the protons on this moiety. The carboxyl ^{13}C was slightly more shielded, while the majority of aliphatic ^{13}C were seldom affected.

Proton Homonuclear Overhauser Effect Spectroscopy (NOESY)

Typically, in the 1D ^{1}H homonuclear NOESY spectra (Fig. 9), the truncated major peaks are the selectively irradiated ones, and the small peaks are the NOEs developed on the adjacent protons. The irradiated peak is negatively phased; therefore, a positive NOE has positive phase; a negative NOE has negative phase. Intermolecular NOEs were not observed between cromolyn and SNAC protons at any concentration combination explored. No cross peaks appeared between cromolyn and SNAC protons using ROESY (Rotating-frame Overhauser Effect Spectroscopy), which measures NOE in the rotating frame. However, with the increase in SNAC concentration, the intramolecular NOEs between cromolyn protons decreased gradually and even exhibited a negative absorption mode when SNAC was present in excess. The change of NOE magnitude and sign was not due to Na^+ from SNAC because NaCl at same molar concentrations failed to induce a comparable effect (data not shown).

FTIR Spectroscopy

The FTIR spectra of cromolyn in D_2O at different concentrations are shown in Fig. 10. The main differences arise at the ring C=O stretch band at around 1625 cm^{-1}. With the increase in cromolyn concentration, the C=O peak showed blue shift.

IR bands from cromolyn and SNAC were largely overlapped due to the existence of several similar functionalities

Table II. ^{13}C Chemical Shifts (ppm) of Cromolyn (10 mM) in D_2O

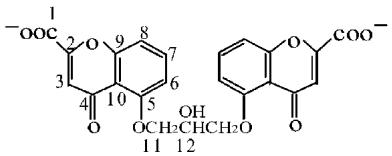

^{13}C Nucleus	δ at 0 mM SNAC	δ at 83 mM SNAC	σ at 167 mM SNAC
1	184.360	184.367	184.360
2	159.538	159.492	159.484
3	115.271	115.348	115.386
4	168.474	168.382	168.321
5	161.272	161.027	160.897
6	112.942	112.377	112.064
7	138.673	138.573	138.497
8	113.859	113.874	113.874
9	160.111	160.187	160.233
10	116.608	116.562	116.539
11	73.816	73.441	73.281
12	70.661	70.562	70.501

Table III. ^{13}C Chemical Shifts (ppm) of SNAC (17 mM) in D_2O

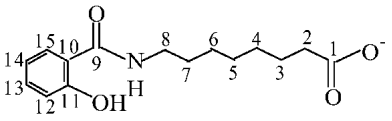

^{13}C nucleus	δ at 0 mM cromolyn	δ at 10 mM cromolyn
1	187.132	187.117
2[a]	28.648	28.656
3[a]	28.892	28.908
4[a]	31.023	31.031
5[a]	31.145	31.145
6[a]	31.451	31.466
7[a]	40.471	40.471
8[a]	42.426	42.418
9	172.697	172.590
10	120.098	119.846
11	160.676	160.745
12	120.320	120.298
13	136.702	136.687
14	122.542	122.474
15	131.180	131.089

[a] Individual aliphatic ^{13}C cannot be assigned accurately. Their overall shifts are compared here.

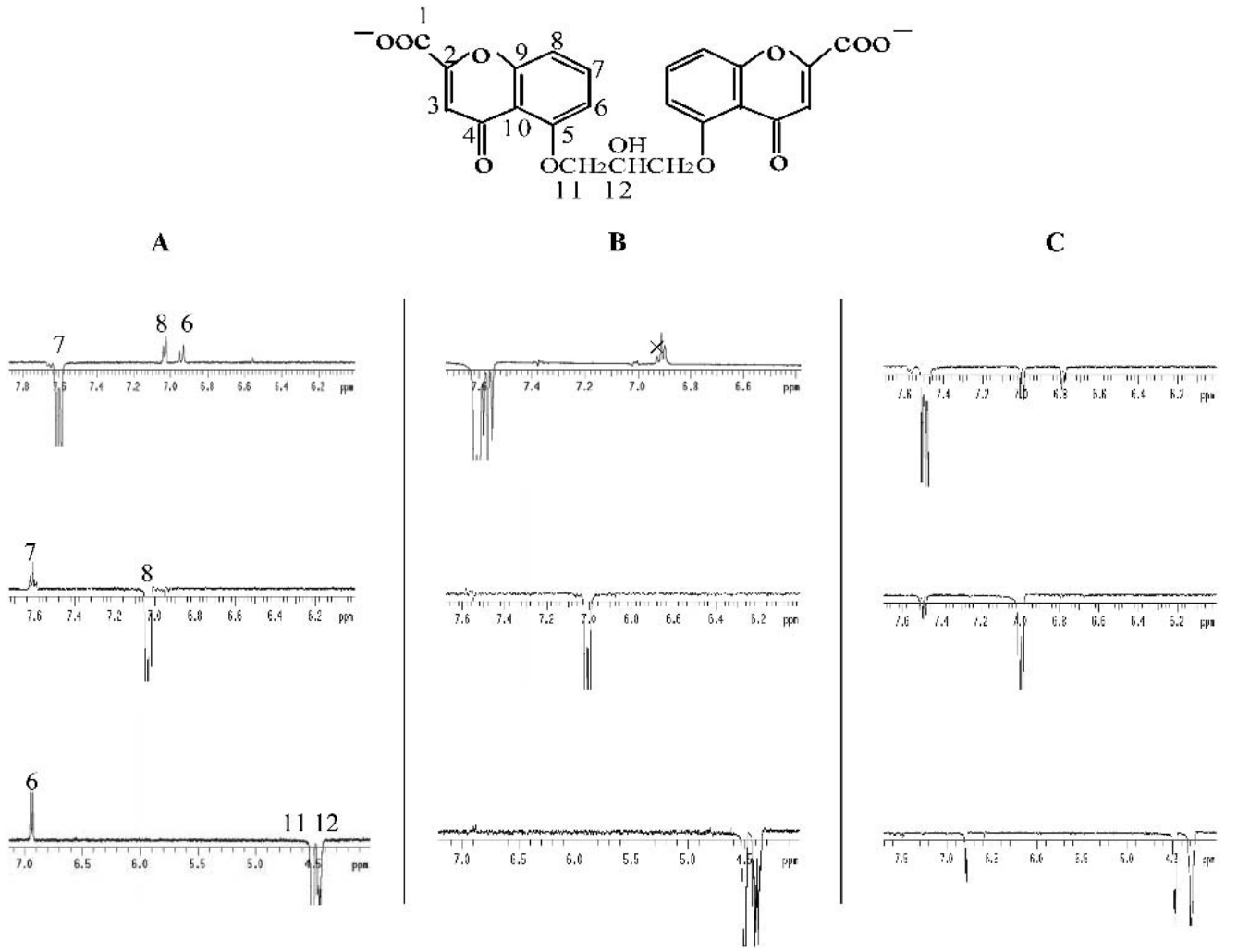

Fig. 9. 1D Homonuclear NOESY of 10 mM cromolyn in the presence of 17 mM (A), 100 mM (B), and 333 mM (C) SNAC in D_2O. The NOE peak denoted with "×" arises from SNAC H14 due to simultaneous irradiation of SNAC H15 peak that is overlapped with cromolyn H7.

(Fig. 11A). Difference spectra were generated by subtracting SNAC data from the cromolyn/SNAC mixture spectra in order to extract spectral changes upon addition of excessive SNAC. As shown in Fig. 11B, a number of spectral changes were observed when the two compounds were mixed in solution. In addition to the blue shift of the cromolyn C=O band, intense new bands around 1545 cm^{-1} and a relatively weaker band near 1400 cm^{-1} appeared in the difference spectra. Bands in those regions were observed in the SNAC FTIR spectrum and could be assigned to amide-II' and asymmetric COO^- stretching (near 1550 cm^{-1}) and symmetric COO^- stretching bands (near 1410 cm^{-1}). We speculate that the new bands in the difference spectrum were from the asymmetric and symmetric COO^- stretching vibrations of SNAC as a consequence of perturbed hydrogen bonding via its interaction with cromolyn.

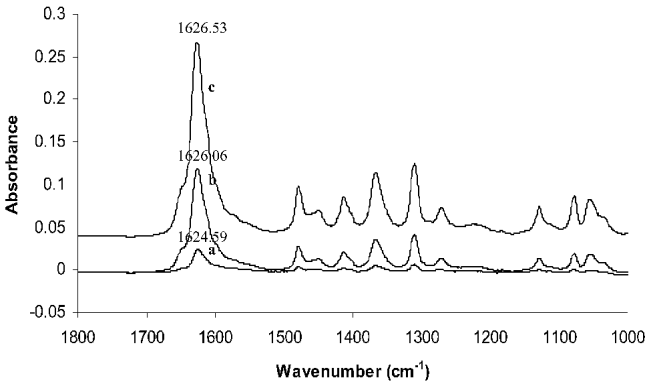

Fig. 10. IR spectra of 10 mM (a), 50 mM (b), and 100 mM (c) cromolyn in D_2O. The peaks of C=O stretching regions are marked by their wavenumbers.

Molecular Dynamics Simulations

Molecular dynamics simulations were carried out in order to visualize and explore potential interactions between cromolyn and SNAC. The predominant type of interaction observed in the simulations was ring stacking. In all simulations carried out, SNAC inserted its aromatic ring in sandwich fashion, i.e., between the two rings of cromolyn (Fig. 12). This was observed both in simulations carried out with one molecule of cromolyn and one molecule of SNAC and in those carried out with two molecules of cromolyn and two molecules of SNAC. Other modes of interaction observed during

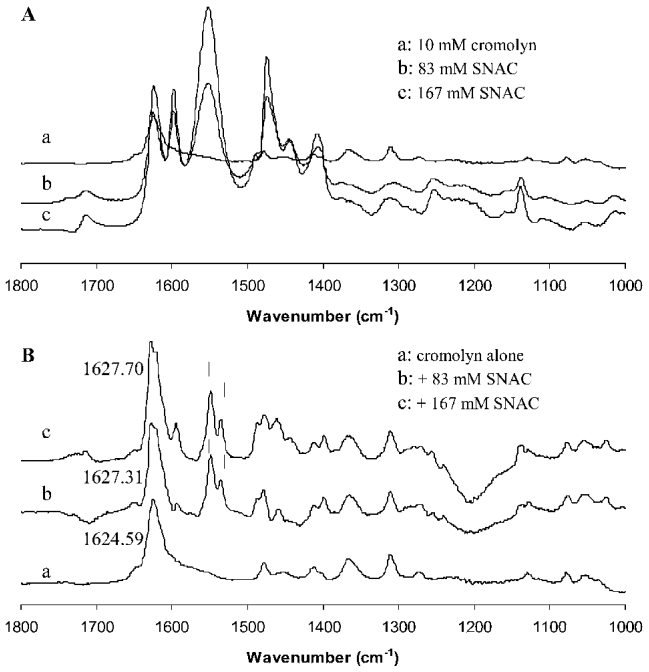

Fig. 11. IR spectra of cromolyn and SNAC in D_2O. Difference spectra of cromolyn and SNAC mixture are compared with spectrum of 10 mM cromolyn in B. The peaks of cromolyn C = O stretching regions are marked by their wavenumbers on the side. New bands are marked by " |" on difference spectra.

the simulations included SNAC's aromatic ring stacked to the external face of one of cromolyn's rings. One of the frames, in which SNAC's 2-hydroxybenzamide ring is inserted between the two aromatic rings of cromolyn as shown in Fig. 12, was used as the starting system to perform a 0.5 ns simulation. During this simulation, the two molecules remained this position most of the time. Occasionally SNAC came out of the space between the two chrome rings and stacked its aromatic ring to the external face of one of cromolyn's rings, but later returned to the starting position.

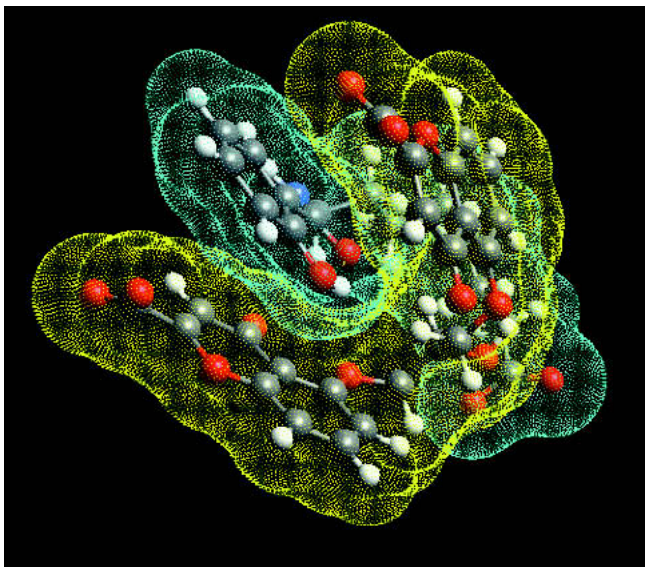

Fig. 12. Noncovalent complex obtained during molecular dynamics simulations of cromolyn (yellow) and SNAC (blue). The 2-hydroxybenzamide ring of SNAC is in between the two aromatic rings of cromolyn. The interaction between the two molecules is predominatly van der waals driven by ring stacking.

DISCUSSION

For a drug to be absorbed orally, it must possess certain physicochemical properties, that is, appropriate hydrophilicity to dissolve in the gastrointestinal fluids, and sufficient hydrophobicity to diffuse effectively across the gastrointestinal epithelium. Cromolyn is rather hydrophilic, containing strong acidic twin carboxyl groups (pKa = 2.0) (26) and high hydrogen bonding capability. These structural features contribute to its extreme hydrophilicity [*n*-octanol/neutral aqueous buffer distribution coefficient less than 0.001 (4)] and corresponding low membrane permeability, which render its oral absorption almost negligible.

The moderate but significant increase of cromolyn's permeation observed in our Caco-2 monolayer experiments when added in combination with SNAC is in agreement with the extent of the oral bioavailability increase observed *in vivo* when coadministered with this delivery agent, both in animal models and in humans (12,16). The oral bioavalability of highly hydrophilic drugs like cromolyn may never reach high levels. Nevertheless, moderate increases, such as those observed in our Caco-2 experiments as well as in preclinical and clinical studies may be sufficient to develop oral forms.

SNAC significantly increased cromolyn's permeation across Caco-2 cell monolayers without affecting the permeation of paracellular and transcellular markers such as fluorescein and theophylline. These results are in agreement with previous studies conducted in our laboratories, which showed that SNAC at 83 mM, and even higher concentrations, did not significantly increase the absorption of paracellular and transcellular markers such as [^{14}C]-mannitol and [^{3}H]-hydrocortisone (13). The absence of tight junction or membrane disruption was also confirmed in recent microscopy studies (15). These results indicate that SNAC enhances the absorption of cromolyn through a specific mechanism that does not involve the opening of tight junctions or damage to the cell membrane. In addition, SNAC shows some selectivity with respect to the molecule it transports, facilitating the absorption of cromolyn but not that of fluorescein or theophylline. These features clearly differentiate SNAC from compounds that function as classic absorption enhancers. Absorption enhancers, such as medium chain fatty acids, EDTA, bile salts, or surfactants (27–29), increase the absorption of molecules with low permeation by opening tight junctions between cells and/or by disrupting cell membranes. This may pose a number of concerns with respect to safety (30). In addition, absorption enhancers often show high variability due to the lack of a specific mechanism and absorption pathway. Sodium caprylate, which is known to open tight junctions and disrupt the cell membrane (31), increased Caco-2 permeability to paracellular and transcellular markers as well as cromolyn, with high variability in all cases. SNAC on the other hand, enhanced the absorption of cromolyn with less variability and without altering the permeation of paracellular and transcellular markers. This indicates that SNAC transports cromolyn through a selective mechanism.

Previous studies indicated that the mechanism of SNAC-mediated drug transport involves non-covalent interaction between SNAC and the transported drugs (8,9,12). Such in-

teraction presumably increases the drug hydrophobicity and, consequently, its passive absorption. Results from the ITC experiments reported here indicate that SNAC weakly interacts with cromolyn via its 2-hydroxybenzamide moiety.

The results from the ITC and NMR studies indicate that SNAC interacts with cromolyn via its 2-hydroxybenzamide moiety. NMR data further suggest that the interaction must be primarily localized to the area between the isopropyl linkage and the adjacent ring nuclei including the carbonyl groups on cromolyn. The atoms of these cromolyn and SNAC moieties are the ones that experienced substantial chemical shifts when the two compounds were together in solution. These findings are in agreement with the representative result from molecular dynamics simulations.

SNAC disrupts cromolyn's self-association (Fig. 7). This is due to the fact that ring stacking is an important driving force for both cromolyn self-association and cromolyn/SNAC interaction. Thus, SNAC and cromolyn may compete for the same binding sites. Nevertheless, cromolyn/SNAC interaction is strong enough to compete with and displace cromolyn/cromolyn interaction.

The NOE phenomenon is a manifestation of cross-relaxation between two nuclear spins that are mutually close (usually <0.5 nm) in space. This indicates the existence of intermolecular or intramolecular interactions. Under otherwise similar conditions (e.g., temperature, pH, solvent), the magnitude and sign of NOEs are dependent on the molecular tumbling rate. Zero NOEs can indicate absence of intermolecular interactions or could be due to the fact that the molecular motion, measured by tumbling rate, falls into the intermediate region. In the latter case, measurement of NOEs in the rotating-frame provides an alternative solution for determining the existence of intermolecular interactions (32). In order to observe intermolecular NOEs between a substrate and a ligand, the complex must be sufficiently populated, and there must be a significant probability of a cross-relaxation event occurring between the nuclei of interest during the lifetime of the complex (33). The absence of both intermolecular NOEs and cross peaks in the ROESY spectra imply that these conditions are not fulfilled in the case of SNAC and cromolyn mixture under our experimental conditions. Nevertheless, the NOE sign change observed at high SNAC concentrations indicates that cromolyn and SNAC form complexes large enough to significantly restrict the molecular motion of cromolyn. These changes in cromolyn's NOEs induced by SNAC also suggest that the size and the fraction of the complexes, increase with SNAC concentration.

The chemical shifts shown in Table I indicate that Na^+ and K^+ facilitate or stabilize the interaction between cromolyn and SNAC. This could be due to a reduced electrostatic repulsion between the carboxyl groups of both compounds at high ionic strengths. Some of these shifts could also be attributed to increased cromolyn self-association. For example, the shift of H7 could stem solely from increased self-association of cromolyn. If this were the case, H3 should exhibit a significant upfield shift, as evidenced in our previous study (25). Yet, the H3 resonance was barely affected by the increase in NaCl or KCl concentration. Most likely Na^+ and K^+ stabilize both cromolyn self-association and cromolyn/SNAC interaction. Increased cromolyn self-association leads to an upfield shift of the H3, which is counteracted by a downfield shift due to increased cromolyn/SNAC interaction. The overall result is therefore a minimal change in the H3 resonance. The spectra obtained at different pDs support this hypothesis. Basic pDs are expected to destabilize cromolyn/SNAC interaction due to the deprotonation of the phenoxyl group of SNAC but should not affect cromolyn self-association. Consequently, the downfield shift of H3 caused by cromolyn/SNAC interaction should decrease with the increase in pD, whereas the upfield shift due to cromolyn/cromolyn interaction should not change. The result should be an upfield shift of H3 with the pH increase. This was precisely what we observed.

Water plays an important role not only in holding a planar conformation of cromolyn molecules in dilute solution but also in maintaining the crystal lattice of solid cromolyn (34,35). X-ray crystallographic studies revealed unique structural features of cromolyn hydrates including a water-filled "channel" located in the large space between the two identical rings (35,36). This space is identified as the location of the secondary hydration structure with 9 potential sites for hydration (carboxyl, ether, hydroxyl and carbonyl groups) apart from the sodium ions (37). The X-ray pattern given by the middle liquid crystal phase is interpreted by a model in which the planar cromolyn molecules are clustered into rods separated by such a water-filled "channel," and with the polar carboxyl groups pointing outward. Upon dilution the average water separation increases until a break-up of the rods takes place by translations and rotations of the planar molecules (37). Cromolyn/SNAC interaction identified in this study can increase the overall hydrophobicity of cromolyn and/or modify the hydration shell of cromolyn in several different ways. In the case of the interaction mode shown in Fig. 12, SNAC displaces the water molecules in the water-filled channel of cromolyn. Any of the other possible ring stacking interactions would also reduce the hydration shell of cromolyn. In addition, since SNAC is more hydrophobic than cromolyn (unlike cromolyn, SNAC is absorbed readily by passive diffusion), the cromolyn/SNAC complexes should be more hydrophobic than cromolyn alone. The observed reduction of cromolyn self-association in the presence of SNAC may also contribute to increase cromolyn's permeation. Results from the FTIR spectra confirmed that the hydration of cromolyn decreases in the presence of SNAC. The blue shift of cromolyn's C = O IR band in the presence of SNAC suggests that the average hydrogen bonding with surrounding water molecules is weaker in the presence of SNAC.

Both the titration calorimetry and NMR results indicate that such interaction is weak and the subsequent complexes are easily dissociated by dilution in the bloodstream after absorption. SNAC and cromolyn probably form various types of complexes with different stoichiometries. Cromolyn/SNAC interaction can increase cromolyn's overall hydrophobicity and reduce its hydration shell. The formation of these hydrophobic Cromolyn/SNAC complexes could explain the increased cromolyn permeation across the intestinal epithelium observed in the presence of SNAC.

ACKNOWLEDGMENTS

The authors thank Heather Tang and Klavdiya Burdukovskaya for their assistance in culturing the cells. The work was funded by Emisphere Technologies, Inc. NMR data were obtained through the Analytical Instrumentation Center of the School of Pharmacy, University of Wisconsin-Madison.

REFERENCES

1. G. G. Shapiro and P. Kőnig. Cromolyn Sodium: a review. *Pharmacotherapy* **5**:156–170 (1985).
2. B. J. Undem and L. M. Lichtenstein. Drugs used in the treatment of asthma. In J. G. Hardman, L. E. Limbird, and A. G. Gilman (eds.), *The Pharmacological Basis of Therapeutics*, 10th ed., McGraw-Hill, New York, 2001, pp 733–754.
3. Fisons Corporation. Intal-cromolyn sodium: a monograph. Fisons Corp., Bedford, MA, 1973.
4. T. Mori, K. Nishimura, S. Tamaki, S. Nakamura, H. Tsuda, and N. Kakeya. Pro-drugs for the oral delivery of disodium cromoglycate. *Chem. Pharm. Bull. (Tokyo)* **36**:338–344 (1988).
5. A. Yoshimi, H. Hashizume, S. Tamaki, H. Tsuda, F. Fukata, K. Nishimura, and N. Yata. Importance of hydrolysis of amino acid moiety in water-soluble prodrugs of disodium cromoglycate for increased oral bioavailability. *J. Pharmacobiodyn.* **15**:339–345 (1992).
6. S.-J. Wu and J. R. Robinson. Transcellular and lipophilic complex-enhanced intestinal absorption of human growth hormone. *Pharm. Res.* **16**:1266–1272 (1999).
7. G. M. Mlynek, L. J. Calvo, and J. Robinson. Carrier-enhanced human growth hormone absorption across isolated rabbit intestinal tissue. *Int. J. Pharm.* **197**:13–21 (2000).
8. S. J. Milstein, H. Leipold, D. Sarubbi, A. Leone-Bay, G. M. Mlynek, J. R. Robinson, M. Kasimova, and E. Freire. Partially unfolded proteins efficiently penetrate cell membranes — implications for oral drug delivery. *J. Control. Rel.* **53**:259–267 (1998).
9. A. Leone-Bay, M. Sato, D. Paton, A. H. Hunt, D. Sarubbi, M. Carozza, J. Chou, J. McDonough, and R. A. Boughman. Oral delivery of biologically active parathyroid hormone. *Pharm. Res.* **18**:964–970 (2001).
10. D. Brayden, E. Creed, A. O'Connell, H. Leipold, R. Agarwal, and A. Leone-Bay. Heparin absorption across the intestine: effects of sodium N-[8-(2-hydroxybenzoyl)amino]caprylate in rat *in situ* intestinal instillations and in Caco-2 monolayers. *Pharm. Res.* **14**:1772–1779 (1997).
11. T. M. Rivera, A. Leone-Bay, D. R. Paton, H. R. Leipold, and R. A. Baughman. Oral delivery of heparin in combination with sodium N-[8-(2-hydroxybenzoyl)amino]caprylate. PHARMACOLOGICAL CONSIDERATIONS. *Pharm. Res.* **14**:1830–1834 (1997).
12. A. Leone-Bay, H. Leipold, D. Sarubbi, B. Variano, T. Rivera, and R. A. Baughman. Oral delivery of sodium cromolyn: preliminary studies *in vivo* and *in vitro. Pharm. Res.* **13**:222–226 (1996).
13. S.-J. Wu. Mechanistic studies on the enhanced mucosal transport of human growth hormone by certain amino acid derivatives. Ph.D. Thesis, University of Wisconsin-Madison (1999).
14. B. Li. Noncovalent carrier enhanced protein absorption-cellular and subcellular mechanistic studies. Ph.D. Thesis, University of Wisconsin-Madison (2001).
15. D. Malkov, H. Wang, S. Dinh, and I. Gomez-Orellana. Pathway of oral absorption of heparin with sodium N-c*aprylate. Pharm. Res.* **19**:1180–1184 (2002).
16. M. Goldberg. Oral macromolecule delivery: reviews of the large and expanding clinical database. Winter Symposium & 11th International Symposium on Recent Advances in Drug Delivery Systems, Salt Lake City, Utah, March 3–6, 2003.
17. R. J. Ogg, B. P. Kingsley, and J. S. Taylor. WET, a T1- and B1-insensitive water-suppression method for *in vivo* localized ^{1}H NMR spectroscopy. *J. Magn. Reson. Ser. B.* **104**:1–10 (1994).
18. S. H. Smallcombe, S. L. Patt, and P. A. Keifer. WET solvent suppression and its applications to LC NMR and high-resolution NMR spectroscopy. *J. Magn. Reson. Ser. A.* **117**:295–303 (1995).
19. J. Stonehouse, P. Adell, J. Keeler, and A. J. Shaka. Ultrahigh-quality NOE spectra. *J. Am. Chem. Soc.* **116**:6037–6038 (1994).
20. K. Stott, J. Stonehouse, J. Keeler, T.-L. Hwang, and A. J. Shaka. Excitation sculpting in high-resolution nuclear magnetic resonance spectroscopy: application to selective NOE experiments. *J. Am. Chem. Soc.* **117**:4199–4200 (1995).
21. K. Stott, J. Keeler, Q. N. Van, and A. J. Shaka. One-dimensional NOE experiments using pulsed field gradients. *J. Magn. Reson.* **125**:302–324 (1997).
22. W. Hoover. Canonical Dynamics: Equilibrium Phase-space Distributions. *Phys. Rev.* **A31**:1695–1697 (1985).
23. S. Nose. A unified formulation of the constant temperature molecular dynamics methods. *J. Chem. Phys.* **81**:511–519 (1984).
24. G. A. Stephenson and B. A. Diseroad. Structural relationship and desolvation behavior of cromolyn, cefazolin and fenoprofen sodium hydrates. *Int. J. Pharm.* **198**:167–177 (2000).
25. X. Ding, T. C. Stringfellow, and J. R. Robinson. Self-association of cromolyn sodium in aqueous solution characterized by nuclear magnetic resonance spectroscopy. *J. Pharm. Sci.* **93**:1351–1358 (2004).
26. H. S. White. Histamine and antihistamine drugs. In *Remington: The Science and Practice of Pharmacy*, 20th ed., Lippincott Williams & Wilkins, Philadelphia, 2000, pp. 1464–1476.
27. V. H. L. Lee, A. Yamamoto, and U. B. Kompella. Mucosal penetration enhancers for facilitation of peptide and peptide drug absorption. *Crit. Rev. Ther. Drug Carrier Syst.* **8**:91–192 (1991).
28. B. J. Aungst, H. Siatoh, D. L. Burcham, S.-M. Huang, S. A. Mousa, and M. A. Hussain. Enhancement of the intestinal absorption of peptides and non-peptides. *J. Control. Rel.* **41**:19–31 (1996).
29. J. A. Fix. Strategies for delivery of peptides utilizing absorption-enhancing agents. *J. Pharm. Sci.* **85**:1282–1285 (1996).
30. J. R. Robinson and X. Yang. Absorption Enhancers. In J. Swarbrick and J.C. Boylan (eds.), *Encyclopedia of Pharmaceutical Techniques,* vol. 18, Marcel Dekker, Inc., New York, 1999, pp. 1–27.
31. T. Sawada, T. Ogawa, M. Tomita, M. Hayashi, and S. Awazu. Role of Paracellular pathway in nonelectrolyte permeation across rat colon epithelium enhanced by sodium caprate and sodium caprylate. *Pharm. Res.* **8**:1365–1371 (1991).
32. T. D. W. Claridge. *High-Resolution NMR Techniques in Organic Chemistry*, Pergamon Press, Oxford, 1999, pp. 277–339.
33. H. Mo and T. Pochapsky. Intermolecular Interactions characterized by nuclear overhauser effects. *Progr. NMR Spectrosc.* **30**:1–38 (1997).
34. J. S. G. Cox, G. D. Woodard, and W. C. McCrone. Solid state chemistry of cromolyn sodium disodium cromoglycate). *J. Pharm. Sci.* **60**:1458–1465 (1971).
35. L. R. Chen, V. G. Young Jr., D. Lechuga-Ballesteros, and D. J. W. Grant. Solid-state behavior of cromolyn sodium hydrates. *J. Pharm. Sci.* **88**:1191–1200 (1999).
36. S. Hamodrakas, A. J. Geddes, and B. Sheldrick. X-ray analysis of disodium cromoglycate. *J. Pharm. Pharmacol.* **26**:54–56 (1974).
36. S. A. Attiga, D. D. Eley, and M. J. Hey. A nuclear magnetic relaxation study of bound water in solutions of disodium cromoglycate. *J. Pharm. Pharmacol.* **31**:387–391 (1979).
37. N. H. Hartshorne and G. D. Woodard. Mesomorphism in the system disodium cromoglycate-water. *Mol. Cryst. Liq. Cryst.* **23**:343–368 (1973).